Application of Imperialist Competitive Algorithm with its Enhanced Approaches for Multi-objective Optimal Reactive Power Dispatch Problem

Gonggui Chen, Jia Cao, Zhizhong Zhang*, and Zhi Sun

***Abstract*— This study proposes three enhanced multi-objective imperialist competitive algorithms: MOICA-I, MOICA-II and MOICA-III for solving multi-objective optimal reactive power dispatch (MOORPD) problem. In MOICA-I, the fuzzy power method is proposed to solve the application of imperialist competitive algorithm (ICA) in multi-objective problems (MOPs). In MOICA-II, based on the non-dominated sorting method and the crowded distance calculation, the constraint dominant method and the total rank method are proposed to solve the inequality constraint and the ranking of the solutions. In MOICA-III, combined with the fuzzy power method in MOICA-I and the constraint dominant method in MOICA-II, the power quantitation method is proposed to solve the above three problems simultaneously: the application of the ICA, the processing of the constraint and the measurement method of the solutions. In order to verify the effectiveness of the enhanced approaches for the MOORPD problem, three objective functions including total active power losses, voltage deviation and voltage stability index are considered. Simulation experiments are carried out in the IEEE 30, 57 and 118 bus systems. The results show that the enhanced approaches can effectively solve the MOORPD problem, and the performance of MOICA-III is outstanding.**

***Index Terms*—Multi-objective optimal reactive power dispatch; imperialist competitive algorithm; fuzzy power method; constraint dominant method; power quantitation method**

I. Introduction

THE optimal reactive power dispatch (ORPD) problem is a sub-problem of optimal power flow (OPF) problem, and it is also one of the important research issues of power system optimization [1]–[3]. The main purpose of ORPD is to improve the power flow distribution of the power system by adjusting the control device under certain constraints, thereby strengthening the safe operation of the power grid, improving the system voltage quality and reducing the operating cost of the power grid. In the ORPD problem, these control devices (variables) mainly include three categories: the generator voltages, the transformer taps and the reactive power compensation [4], [5]. In addition, the generator voltages are continuous variables, the other two variables are discrete variables. Therefore, from the perspective of the mathematical model, the ORPD problem is a non-convex, non-differentiable, nonlinear, multi-constrained and high-dimensional optimization problem. According to the number of optimization targets, the ORPD problem can be divided into single-objective ORPD (SOORPD) problem and multi-objective ORPD (MOORPD) problem [6]–[8].

Different from the single-objective optimization problems (SOPs), the multi-objective optimization problems (MOPs) need optimize multiple targets simultaneously, and seek a set of Pareto optimal solution sets, and then find the best compromise solution (BCS) from these solution sets [9]. Therefore, the solution of MOPs is generally more difficult. The traditional methods for solving MOPs include linear weighted sum method, ε-constraint method, multi objective programming approach, and goal attainment method [10]–[13]. Although these methods inherit the ideas of some classical algorithms for solving SOPs, they have a common flaw, which means, these methods must be run multiple times to get the Pareto optimal solution sets of the original problem. And the above methods are difficult to deal with non-differentiable, non-convex and large-scale problems which lead to the limitation of the practical application of these methods.

The successful application of multi-objective evolutionary computation approach in the field of the multi-objective optimization provides a new research direction for MOPs. Since the evolutionary algorithm can obtain multiple Pareto solutions in a single simulation run and can easily process discontinuous or concave Pareto fronts, this method has unique advantages in solving the MOPs. In recent years, a large number of algorithms have been proposed and applied to solve the MOPs, such as non-dominated sorting genetic algorithm II (NSGA-II), non-dominated sorting genetic algorithm III (NSGA-III), strength Pareto evolutionary algorithm 2 (SPEA2), Pareto envelope-based selection algorithm II (PESA-II) and multi objective particle swarm optimization (MOPSO) [14]–[16]. Since the imperialist

Manuscript received January 23, 2019; revised April 18, 2019. This work was supported by Innovation Team Program of Chongqing Education Committee (CXTDX201601019), Chongqing University Innovation Team under Grant (KJTD201312) and the National Natural Science Foundation of China (Nos. 51207064 and 61463014).

Gonggui Chen is with the Key Laboratory of Network control & Intelligent Instrument, Chongqing University of Posts and Telecommunications, Ministry of Education, Chongqing 400065, China; Key Laboratory of Complex Systems and Bionic Control, Chongqing University of Posts and Telecommunications, Chongqing 400065, China(e-mail:chenggpower@126.com).

Jia Cao is with the Key Laboratory of Complex Systems and Bionic Control, Chongqing University of Posts and Telecommunications, Chongqing 400065, China (e-mail: caojia1995@126.com).

Zhizhong Zhang is with the Key Laboratory of Communication Network and Testing Technology, Chongqing University of Posts and Telecommunications, Chongqing 400065, China (corresponding author, e-mail: zhangzztx@163.com).

Zhi Sun is with the Chn Energy Enshi Hydropower Co.,Ltd, Enshi 445000, China (e-mail: sunzhi24@126.com).

competitive algorithm (ICA) was proposed by Atashpaz-Gargari and Lucas, it has been successfully applied to a variety of optimization problems [17]. In [18], an enhanced ICA (EICA) is proposed to aim at improving its searching ability. In [19], the researcher proposed the Sigma method for improving multi-objective ICA (MOICA). In [20], a new MOMICA was proposed and applied to solve the multi-objective OPF (MOOPF) problem. In [21], a modified GBICA (MGBICA) is presented for solving the optimal electric power planning problem.

ICA has obvious features such as simple operation, high accuracy and fast searching speed, which makes it have certain advantages and efficiency in solving optimization problems [22]–[24]. The update of ICA mainly depends on the objective function value (power value) of the individual country. However, there are multiple targets in the MOPs that conflict with each other, which makes the originally algorithm cannot directly solve the MOPs. In order to apply ICA to solve the MOOORPD problem, we firstly need to deal with the application of ICA on MOPs. Therefore, this paper proposes a MOICA based on fuzzy power method to solve the application of ICA, and we call this method MOICA-I. In addition, since the MOOORPD problem is a multi-constrained problem, whether the constraint processing method is reasonable has a great influence on the algorithm result. Based on the non-dominated sorting method and the crowded distance calculation method [25], we propose a constraint dominant method for judging the merits of the country, and ranking all the countries according to their merit. Then, we call this method MOICA-II. In order to further quantify the value of country's power and prioritize constraints. Based on the constraint dominant method in the MOICA-II and the fuzzy power method in the MOICA-I, the power quantitation method is proposed, and we call this method MOICA-III.

The aforementioned MOICA-I, MOICA-II and MOICA-III algorithms were tested on the IEEE30 bus system, the IEEE57 bus system and the IEEE118 bus system to verify their effectiveness and performance. In addition, the Generational Distance (*GD*) and Hyper-volume (*HV*) indicators are used to measure the stability and diversity of the three algorithms [26], [27]. For different bus types and target combinations, we conducted simulation experiments in six cases. The simulation results show the effectiveness of the above three enhanced methods, and also verify the superiority of the MOICA-III algorithm.

The following sections of this paper are organized as follows: The mathematical model description of the MOORPD problem is shown in Section II. Section III describes the MOICA-I, MOICA-II and MOCA-III algorithms for solving the MOORPD problems. The simulation results and performance analysis of the algorithms can be seen in Section IV, and Section V provides the final conclusion.

II. MATHEMATICAL MODELING

Generally, the main purpose of MOPs is to optimize multiple conflicting objectives while satisfying equality and inequality constraints, simultaneously. An MOP containing *M* objective functions can be mathematically described as follows:

$$\min F(x,u) = [\, f_1(x,u),\, f_2(x,u), \cdots,\, f_M(x,u)] \tag{1}$$

subject to:

$$g(x,u) = 0 \tag{2}$$

$$h(x,u) \le 0 \tag{3}$$

where F is the objective functions, g and h are constraints. In the MOORPD problem, x is the vector of state variables consisting of: the load bus voltages V_L, the generator reactive power outputs Q_G and the transmission line loadings S_L. Therefore, the x can be expressed as follows:

$$x^T = [[V_L]^T, [Q_G]^T, [S_L]^T] \tag{4}$$

u is the vector of control variables consisting of: the generator bus voltages V_G, the transformer taps T and the reactive power compensation Q_C. Thus, the u can be expressed as follows:

$$u^T = [[V_G]^T, [T]^T, [Q_C]^T] \tag{5}$$

where '^{T}' represents transposition.

A. Objective functions of MOORPD

1) Active power losses minimization

This objective of ORPD problem is to minimize the total active power transmission losses in the power system. The objective function are expressed as follows:

$$f_1(x,u) = \min P_{loss} = \sum_{k \in N_E} g_k (V_i^2 + V_j^2 - 2V_iV_j \cos\delta_{ij}) \tag{6}$$

where P_{loss} is the total power losses of the power system; N_E is the number of transmission lines; g_k is the conductance of the kth branch which connects the bus i and bus j; V_i and V_j are the voltage magnitude of bus i and bus j, respectively; δ_{ij} is the voltage angle between bus i and bus j.

2) Voltage deviation minimization

This objective is to minimize the total voltage deviations in all load buses which can be expressed as:

$$f_2(x,u) = \min V_d = \sum_{i=1}^{N_{PQ}} \left| V_i - V^{REF} \right| \tag{7}$$

where V_d is the total voltage deviations; N_{PQ} is the number of PQ buses; V_i is the bus voltage at the ith load node; V^{REF} is the desired voltage magnitude.

3) Voltage stability index minimization

Voltage stability is the capacity of a power system to maintain constant bus voltage when the system is in normal operating conditions or is being subjected to disturbances. In this paper, the voltage stability enhancement is achieved by minimizing voltage stability index (*L index*) and it can be represented by following equations:

$$f_3(x,u) = \min(L\,index) \tag{8}$$

where

$$L\,index = \max(L_j), \quad j \in N_{PQ} \tag{9}$$

and

$$\begin{cases} L_j = \left| 1 - \sum_{i=1}^{N_{PV}} F_{ji} \dfrac{V_i}{V_j} \right|, \quad j \in N_{PQ} \\ F_{ji} = -[\mathrm{Y_{LL}}]^{-1}[\mathrm{Y_{LG}}] \end{cases} \tag{10}$$

where N_{PV} is the number of PV buses; Y_{LL} and Y_{LG} are the sub-matrices. And the Y-bus matrix (node admittance matrix) acquired after separating the PQ buses and PV buses can be stated as:

$$\begin{bmatrix} I_L \\ I_G \end{bmatrix} = \begin{bmatrix} Y_{LL} & Y_{LG} \\ Y_{GL} & Y_{GG} \end{bmatrix} \begin{bmatrix} V_L \\ V_G \end{bmatrix} \quad (11)$$

where I_G and I_L are the currents of PQ buses and PV buses; V_G and V_L are the voltages of PQ buses and PV buses.

B. Constraints of MOORPD

1) Equality constraints

The aforementioned g is equality constraints and it includes:

$$P_{Gi} - P_{Di} - V_i \sum_{j \in N_i} V_j (G_{ij} \cos\delta_{ij} + B_{ij} \sin\delta_{ij}) = 0,\ i \in N \quad (12)$$

$$Q_{Gi} - Q_{Di} - V_i \sum_{j \in N_i} V_j (G_{ij} \sin\delta_{ij} - B_{ij} \cos\delta_{ij}) = 0,\ i \in N_{PQ} \quad (13)$$

where P_{Gi} and Q_{Gi} are the active and reactive power generation; P_{Di} and Q_{Di} are the active and reactive load demand; V_i and V_j are the voltages of the ith bus and the jth bus, respectively; G_{ij} and B_{ij} are the real part and imaginary part of the ijth element of Y-bus matrix; N_i is the number of buses adjacent to the bus i; N is the number of system buses.

2) Inequality constraints

The aforementioned h is inequality constraints and it includes x (state variables) inequality constraints and u (control variables) inequality constraints. The x inequality constraints are formulated as follows:

$$\begin{cases} V_{Li}^{\min} \le V_{Li} \le Q_{Li}^{\max}, & i = 1, \ldots, N_{PQ} \\ Q_{Gi}^{\min} \le Q_{Gi} \le Q_{Ci}^{\max}, & i = 1, \ldots, N_{PV} \\ S_{Lij} \le S_{Li}^{\max}, & i = 1, \ldots, N_E \end{cases} \quad (14)$$

where V_{Li} is the load bus voltages of the ith load bus; S_{Lij} is the apparent power flow of the ijth transmission line; N_{PV} is the number of PV buses; max and min respectively represent the minimum and maximum value of the variable.

The u inequality constraints can be detailed as follows:

$$\begin{cases} V_{Gi}^{\min} \le V_{Gi} \le V_{Gi}^{\max}, & i = 1, \ldots, N_{PV} \\ T_i^{\min} \le T_i \le T_i^{\max}, & i = 1, \ldots, N_T \\ Q_{Ci}^{\min} \le Q_{Ci} \le Q_{Ci}^{\max}, & i = 1, \ldots, N_C \end{cases} \quad (15)$$

where V_{Gi} is the generator bus voltages of the ith generator bus; T_i is the transformer tap settings of the ith transformer; Q_{Ci} is the reactive power compensation capacity of the ith capacitor bank; N_T is the number of transformers; N_C is the total number of capacitor banks.

III. PROPOSED ALGORITHMS FOR MOORPD PROBLEM

A. Overview of ICA

ICA is a new intelligent optimization algorithm inspired by imperialistic competition [28]. This algorithm starts with an initial population and each of them is called countries. Based on their power, the countries are classified into two types: imperialists and colonies. The imperialists (stronger countries) will take control of colonies (weaker countries) to form empires. Then, the imperialistic competition begins among all the empires. During this competition, weak empires collapse and stronger empires take possession of their colonies. Finally, all countries will be controlled by one empire. The main steps are presented as below.

1) Initialization

ICA starts with a population of size N_{pop}. In an N_{var} dimensional optimization problem, a country is a vector containing N_{var} control variables. The control variables in a country include some socio-political features such as, social beliefs, customs, culture, language and other features. In the MOORPD problem, these socio-political features (control variables) represents generator bus voltages, transformer taps and reactive power compensation. Thus the ith country are expressed as follows:

$$country(i) = [p_{i,1}, p_{i,2}, p_{i,3}, \ldots, p_{i,N_{var}}] \quad (16)$$

where $country(i)$ denotes the candidate solution; p_i represents the control variable that should be optimized.

In order to form the initial empires, the first N_{imp} countries with less cost function values are selected as imperialists and the remaining N_{col} countries will be the colonies which are under control of one of empires. For variables ($p_{i,1}$, $p_{i,2}$, $p_{i,3}, \ldots, p_{i,Nvar}$), the cost function $f(country(i))$ can be evaluated by (17).

$$cost(i) = f(country(i)) = f([p_{i,1}, p_{i,2}, p_{i,3}, \ldots, p_{i,N_{var}}]) \quad (17)$$

2) Formation of empires

In this process, each imperialist will acquire a number of colonies based on its power. In order to proportionally divide the colonies among imperialists, the normalized cost of an imperialist is first calculated by (18).

$$C_n = c_n - \max_i \{c_i\} \quad (18)$$

Where c_n is the cost of nth imperialist and C_n is the normalized cost. Then, the normalized power of each imperialist, p_n, can be evaluated by (19).

$$P_n = | C_n / \sum_{i=1}^{N_{imp}} C_i | \quad (19)$$

When the normalized power of all imperialist are gathered, the initial number of colonies for nth empire, NC_n, can be denoted by (20).

$$NC_n = round\{p_n N_{col}\} \quad (20)$$

3) Assimilation

After forming the empires, the assimilation process begins. The movement of a colony towards its respective imperialist depends on two parameters: the distance parameter β and the direction parameter θ. Fig. 1 shows this assimilation process. In this figure, d presents the distance between imperialist and colony, x is a random variable with steady distribution and it can be defined by (21), θ is the deviation angle with an angle parameter γ and it can be defined by (22).

$$x \sim U(0, \beta \times d) \quad (21)$$

$$\theta \sim U(-\gamma, +\gamma) \quad (22)$$

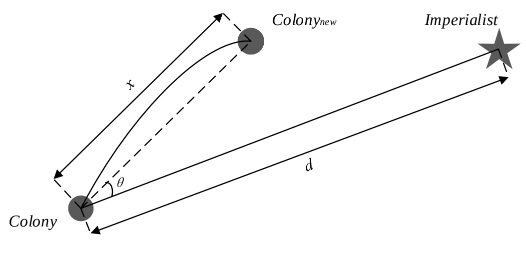

Fig. 1. The assimilation process

4) Revolution

ICA allows all countries to enhance their power through mutation. After assimilation and mutation, a colony may reach to a new position with lower cost (equivalent to having more power than before) than that of imperialist, and then the colony will replace the imperialist.

5) Imperialistic competition

In ICA, this process is modeled by defining the total power of an empire by the power of imperialist and its colonies. The total cost is calculated by following equations:

$$P_{p_n} = |NTC_n / \sum_{i=1}^{N_{imp}} NTC_i| \tag{23}$$

where

$$NTC_n = TC_n - \max_i\{TC_i\} \tag{24}$$

and

$$TC_n = Cost(imp_n) + \xi mean\{Cost(colonies\ of\ emp_n)\} \tag{25}$$

where P_{pn} is the power of each empire, NTC_n is the normalized total cost, TC_n is the total cost of the nth empire and ξ is the colonial weight which is a positive number less than 1.

In the imperialistic competition process, all empires try to take possession of colonies of other empires and control them. Any empire that is not able to succeed in imperialistic competition and cannot increase its power will be eliminated. Ultimately, there exists just one empire and all other countries are its colonies. The position of the imperialist in this empire represents the final solution of the optimization problem.

B. Enhanced approaches

The optimization of the ICA mainly depends on the power of country [28]. In the SOPs, the country's power can be directly determined by the value of the objective function. However, on the contrary to the SOPs with only one single objective, MOPs have two or more objective functions that conflict or interact with each other. Therefore, we cannot directly determine the country's power through the value of objective function. In addition, the MOORPD problem has some obvious features such as multiple constraints and high dimensions, and those features lead to the processing of constraints and the comparison of candidate solutions becomes more complicated. In order to solve these problems encountered in the application of ICA algorithm to MOORPD problem, three MOICAs including MOICA-I, MOICA-II and MOICA-III are proposed.

1) MOICA-I

In MOICA-I, we will redefine the measure of country's power through fuzzy mathematics decision method and we called this approach "fuzzy power method". First, the satisfaction function S_{mi} of the kth cost function f_m of country i is defined as follows:

$$S_{mi}(x) = \begin{cases} 1 & f_{mi} \le f_{m\min} \\ \dfrac{f_{m\max} - f_{mi}(x)}{f_{m\max} - f_{m\min}} & f_{m\min} < f_{mi} < f_{m\max} \\ 0 & f_{mi} \ge f_{m\max} \end{cases} \tag{26}$$

where f_{mmax} and f_{mmin} represent the maximum and the minimum value of the mth cost function, respectively. For every country i, the redefined standardized power can be expressed by the standardized satisfaction function sf_i.

$$sP_i = sf_i = \frac{\sum_{m=1}^{M} S_{mi}}{\sum_{i=1}^{N_p}\sum_{m=1}^{M} S_{mi}} \tag{27}$$

Then, the power of all countries can be represented by sP, which is a fuzzy number between 0 and 1. The country with maximum standardized power value can be seen as the strongest country in this world.

2) MOICA-II

In the MOORPD problem, the constraint violation should be considered before measuring the quality of each candidate solution. The violations of equality constraints are checked by using Newton-Raphson load flow calculation. To solve the problem of constraints, we propose a constraint dominant method. This method can divide all countries into n levels by prioritizing country's constraint violations. Then for the m countries of the same level, the country's power is can be further sorted by the classical crowded distance calculation. Based on the constraint dominant method and the crowded distance calculation, we propose the second improved approach: total rank method.

- *Constraint dominant method*

For the country i, the control variables constraints u_i are handled as follows:

$$u_i = \begin{cases} u_{i,\min} & \text{if} \quad u < u_{i,\min} \\ u_{i,\max} & \text{if} \quad u > u_{i,\max} \\ u_i & \text{if} \quad u_{i,\min} \le u \le u_{i,\max} \end{cases} \tag{28}$$

For each country's state variables, constraint dominant method is proposed which is described as below.

Initially, the power level of all country is divided according to the constraint violation of the state variable, and sum of constraint violations are calculated as follows:

$$Vio(u_i) = \sum_{j=1}^{Ns} \max(h_j(x, u_i), 0) \tag{29}$$

where N_s is the number of particular inequality constraints on state variables.

Next, for control variables u_1 and u_2 from any two different countries, their quality can be judged by the constraint dominant rules:

Constraint Dominant Rules:	
1.	if $Vio(u_1) < Vio(u_2)$ u_1 dominates u_2;
2.	if $Vio(u_1) > Vio(u_2)$ u_2 dominates u_1;
3.	if $Vio(u_1) = Vio(u_2)$
4.	if $f_i(x,u_1) \le f_i(x,u_2)$ for all $i \in \{1, 2, \dots, M\}$ and $f_j(x,u_1) < f_j(x,u_2)$ for any $j \in \{1, 2, \dots, M\}$
5.	u_1 dominates u_2;
6.	else u_2 dominates u_1;

According to the above rules, all countries can be divided into n levels. We can define *Rank* (i) as the power level of country i. The country with the lower rank value is stronger, and the greater the Rank value, the weaker the power.

- *Crowded distance calculation*

All countries can be hierarchically divided by the constraint dominant method. If country i and country j have same rank value, their power strength can be judged by the crowded distance calculation. Then, we define *Dis* (i) as the crowded distance of country i. In current level, the greater the country's crowded distance value is, the stronger the country's power is. Finally, two attributes of a country are obtained: *Rank* (i) and *Dis* (i). For any country i and country j, the total rank relationship can be determined by the following rules:

Total Rank Rules:	
1.	if *Rank* (i) < *Rank* (j) country i is stronger than country j;
2.	if *Rank* (i) > *Rank* (j) country j is stronger than country i;
3.	if *Rank* (i) = *Rank* (j)
4.	if *Dis* (i) > *Dis* (j) country i is stronger than country j;
5.	else country j is stronger than country i;

3) MOICA-III

In the MOICA-II, we have proposed the constraint dominant method to solve the inequality constraint problem and stratify the countries. After the country's rank value is determined, these countries on the rank 1 are considered Pareto-optimal front, and countries with the same rank value are compared by using crowded distance calculation. For any two countries, the crowded distance calculation method can determine which country is stronger, however it cannot determine the difference in power between them.

Based on the constraint dominant method and the fuzzy power method, the third improved method: power quantitation method is proposed. This method can measure the difference in power between all countries. First, calculate the power value of each country by (30).

$$C_i = \sum_{m=1}^{M}\left[\frac{f_m(i)}{\sum_{n=1}^{N_{Rank(i)}} f_m(n)}\right] Rank(i) \times M \qquad (30)$$
$$P_i = 1/C_i$$

Where C_i is the new cost function of country i, P_i is the power of country i, $f_m(i)$ is the mth objective function value of country i, $N_{Rank(i)}$ is the number of those country with same Rank value, $f_m(n)$ is the mth objective function of the nth country with rank value equal to $Rank(i)$.

The cost function consists of two parts: the fuzzy power value and the rank value. In the first part, the objective function values of each country are standardized based on the related objective function values of all countries with same rank, and the value of this part is between 0 and 1. In the second part, *Rank* (i) is greater than or equal to 1, M is greater than 2, thus, the value of second part is greater than 2.

We can observe that the rank value is a dominant factor. The fuzzy power value is a secondary factor, and this factor mainly affects those countries with same rank value. This means that the constraint is always the primary factor determining the country's power. For these countries with the same constraint violations, the power can be differentiated by fuzzy power values rather than just sorting. Therefore, the application of the ICA, the processing method of constraints, and the measurement method of the quality of the solution are simultaneously solved by this method.

C. Proposed algorithms for MOORPD problem

The main goal of this study is solving MOORPD problem using those improved MOICA methods. Using the proposed methods, a set of solutions will stored in a repository (N_R). As the algorithm iterates, the particles in the repository are continually updated, but the size of the repository remains the same. In this section, we employ the MOICA-I, MOICA-II and MOICA-III to solve the MOORPD problem.

Proposed Approaches for MOORPD Problem	
Step1:	Input the needed information of systems and algorithms.
Step2:	Create the initial population (countries). The population dimension is $N_{pop} \times N_{var}$.
Step3:	For each country, calculate the objective functions and constraint violations using Newton-Raphson load flow calculation.
Step4:	Determine country's power by using MOICA-I, MOICA-II or MOICA-III.
Step5:	Store powerful solutions in repository.
Step6:	Form the empires and start assimilation process.
Step7:	Execute revolution operation.
Step8:	Imperialistic competition and eliminate weak empire.
Step9:	Calculation of power value of all countries using MOICA-I, MOICA-II or MOICA-III.
Step10:	Update powerful solutions in repository and keep the repository size constant.
Step11:	Check stopping condition and go to next step if satisfying the preprogrammed maximum generations, otherwise, continue Step7.
Step12:	Output Pareto optimal solutions in repository.
Step13:	Calculation of power value of all Pareto optimal solutions using power quantitation method, choose a Pareto optimal solution with maximum power value as the best compromise solution.

IV. Simulation Results

In order to verify the effectiveness and performance of modified methods, the proposed MOICA-I, MOICA-II and MOICA-III algorithms have been examined and tested in the IEEE 30 bus test system (system 1), the IEEE 57 bus test system (system 2) and the IEEE 118 bus test system (system 3) for solving MOORPD problem. Three objective functions are considered: P_{loss}, V_d and *L index*. Those algorithms have been implemented in MATLAB 2014a and run them on a PC with Intel(R) Core(TM) i5-7500 CPU @ 3.40GHz with 3.41GHz.

A. Parameter settings

1) System parameters

The single line diagram of the system 1 is shown in Fig. 2. Its detail data are given in [29]. The reactive power generation limits and the transmission apparent power flow limits can be seen in [30]. The system 1 has a set of control variables with a 19-dimensional vector. The limits of generator bus voltages are set at 0.95-1.1 in p.u. and the limits of transformer taps are 0.9 and 1.1.

The single line diagram of system 2 is shown in Fig. 3. Its detail data are taken from [31]. The reactive power generation limits and the transmission apparent power flow limits can be seen in [32]. The system 2 has a set of control variables with a 27-dimensional vector. The limits of generator bus voltages are set at 0.9-1.1 in p.u. and the lower and upper limits of transformer taps are 0.9 and 1.1.

To verify the effectiveness of the proposed methods in a larger scale system, these algorithms are tested on the system 3. The single line diagram of system 3 is shown in Fig. 4. Its detail data are taken from [31]. The improved reactive power generation limits and the transmission apparent power flow limits can be found in [33]. The system 3 has a set of control variables with a 75-dimensional vector. The limits of generator bus voltages are set at 0.9-1.1 in p.u. and the minimum and maximum values of transformer taps are 0.9 and 1.1.

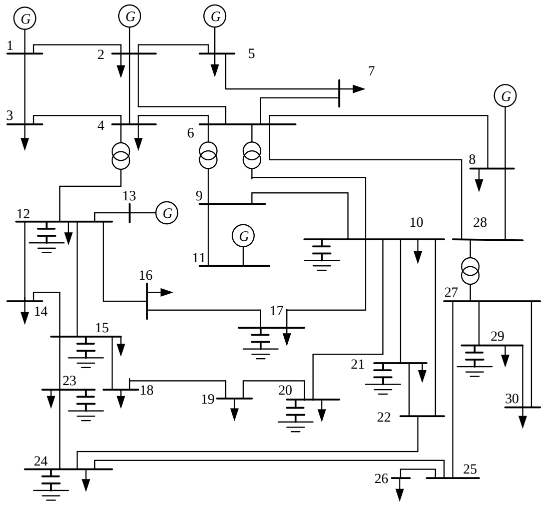

Fig. 2. The single line diagram of the system 1

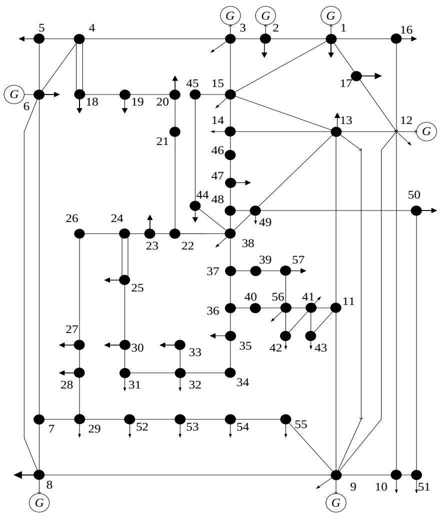

Fig. 3. The single line diagram of the system 2

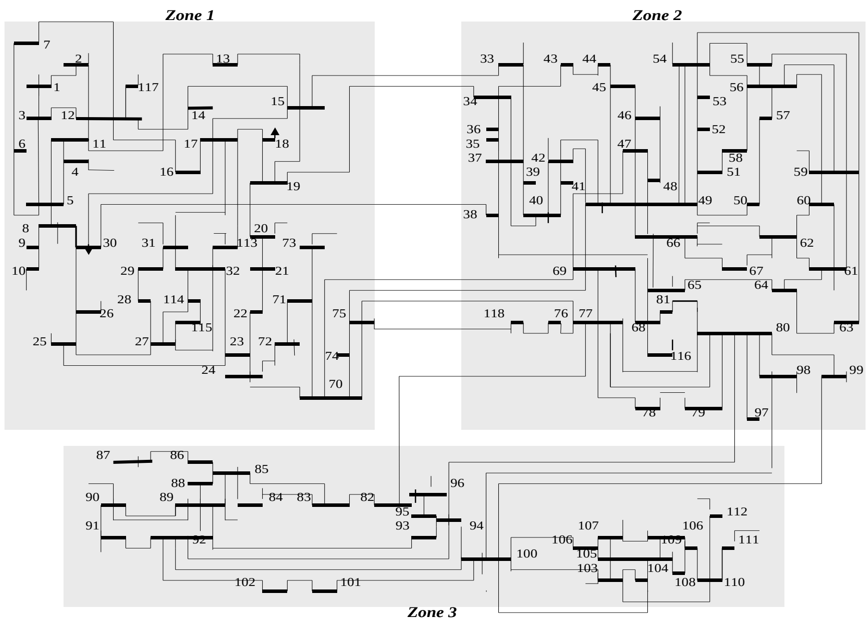

Fig. 4. The single line diagram of the system 3

2) Algorithm parameters

The number of particles and iterations will directly affect the complexity of the optimization problem [34]. Therefore, finding the appropriate parameters is of great significance to this experiment. After a lot of repeated trails, the algorithm parameters are set as shown in TABLE I.

TABLE I SIMULATION PARAMETERS SELECTION

Algorithms	Parameters	Cases 1-5	Case6
MOICA-I	Population size: N_{pop}	80	80
MOICA-II	Repository size: N_R	80	80
MOICA-III	Maximum iterations: K_{max}	300	500
	Number of empires: N_{imp}	16	16
	Number of colonies: N_{col}	64	64
	Deviation angle: θ	$\pi/5$	$\pi/5$
	Distance parameter: β	$\pi/5$	$\pi/5$
	Colonial weight: ξ	2	2

B. Results for system 1

1) Case1: Optimizing P_{loss} and V_d

In this simulation process, the distributions of the Pareto optimal solutions of different methods are shown in Fig. 5. We can observe that the proposed algorithms can obtain the Pareto front. It also shows that the MOICA-III methods can found better BCS. Fig. 6 shows the details of the Pareto front of the MOICA-III, including minimum P_{loss} (MP), minimum V_d (MV) and BCS. And the detailed data of BCS can be seen in TABLE II, it is observed that the BCS of MOICA-III are better than MOICA-I, MOICA-II.

2) Case2: Optimizing P_{loss} and L index

L index is an important indicator for evaluating the stability of the power systems. Thus in case 2, the P_{loss} and *L index* are considered simultaneously. The simulation results of proposed improved methods illustrated in Fig. 7-8. The control variables of BCS of three algorithms are presented in TABLE III. It is found that P_{loss} and *L index* are 0.0513653 p.u. and 0.1207811 for MOICA-III method. Compared with MOICA-I and MOICA-II, the P_{loss} is reduced about 0.0000248 p.u. and 0.0000119 p.u., and the *L index* is reduced about 0.0003926 and 0.0000034. To further verify the performance of the MOICA-III algorithm, we compared it with the reported MOCIPSO algorithm. From the comparisons of the MP, minimum *L index* (ML) and BCS obtained from MOICA-III with the reported MOCIPSO in TABLE IV, the P_{loss} of BCS and the MP are better than MOCIPSO.

3) Case3: Optimizing V_d and L index

In Case3, the performance of the MOICA-I, MOICA-II and MOICA-III for simulation optimization of V_d and *L index* is considered. The distribution of Pareto optimal solution of three methods are shown in Fig. 9-10. We can see from the Fig. 10 that the minimum V_d is 0.179703 p.u. and the minimum *L index* is 0.116921. The simulation results of BCS are given in TABLE V. As seen in TABLE V, the V_d and *L index* of the MOICA-III method can be reduced about 0.0052018 p.u. and 0.0001359 less than the MOICA-II method, and those optimization indicators of the MOICA-II method can be reduced about 0.0124589 p.u. and 0.0001341 less than the MOICA-I method.

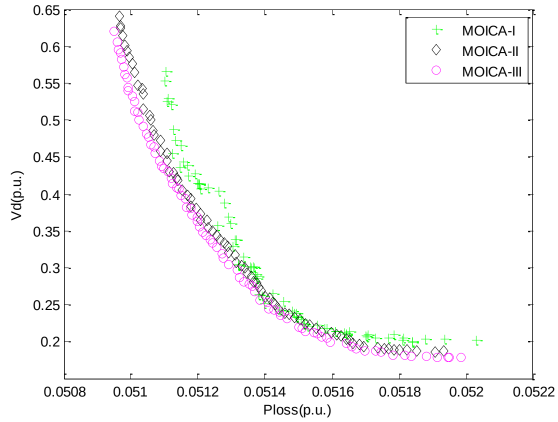

Fig. 5. Simulation results obtained for case1 using of MOICA-I, MOICA-II, MOICA-III

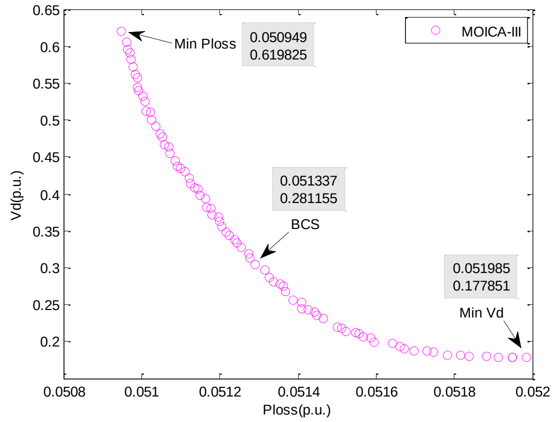

Fig. 6. Pareto optimal fronts of MOICA-III in case1

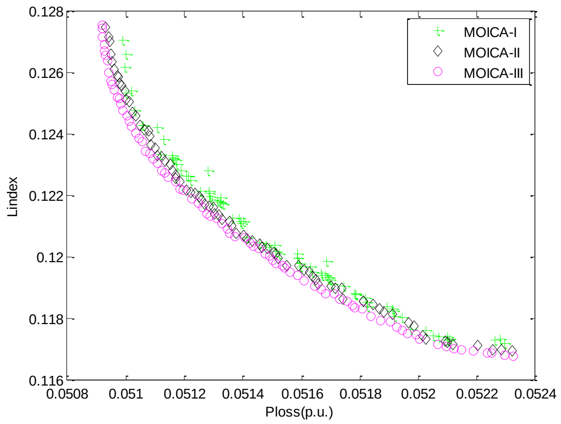

Fig. 7. Simulation results obtained for case2 using of MOICA-I, MOICA-II, MOICA-III

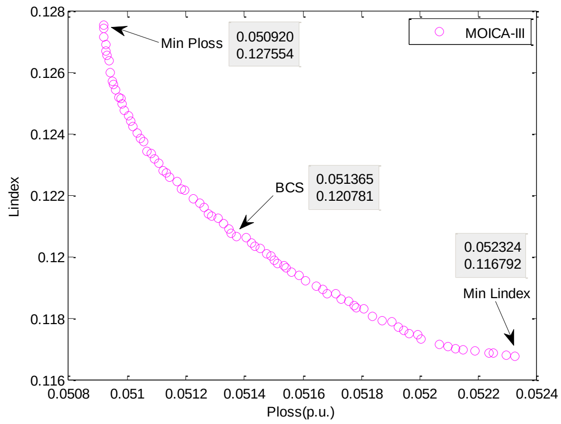

Fig. 8. Pareto optimal fronts of MOICA-III in case2

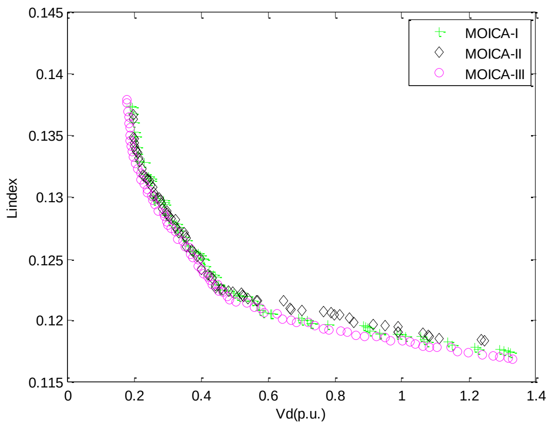

Fig. 9. Simulation results obtained for case3 using of MOICA-I, MOICA-II, MOICA-III

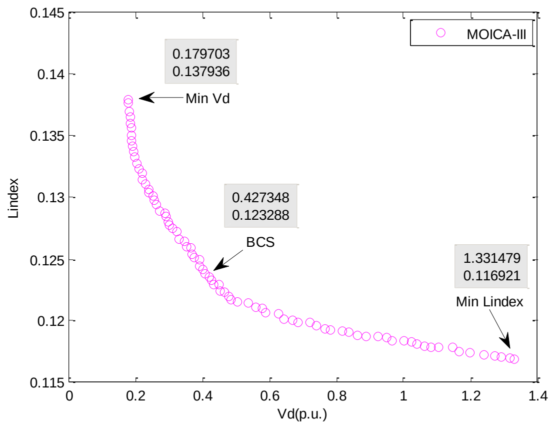

Fig. 10. Pareto optimal fronts of MOICA-III in case3

TABLE II SIMULATION RESULTS OF BCS OF CASE1

Control Variables	MOICA-I	MOICA-II	MOICA-III	Control Variables	MOICA-I	MOICA-II	MOICA-III
V_{G1}(p.u.)	1.07930	0.97652	1.02930	C_{10}(p.u.)	0.04930	0.02360	0.04420
V_{G2}(p.u.)	1.10000	0.97140	1.01072	C_{12}(p.u.)	0.04430	0.00360	0.00000
V_{G5}(p.u.)	0.95000	1.02526	0.98946	C_{15}(p.u.)	0.04380	0.03290	0.03600
V_{G8}(p.u.)	1.08979	0.97368	1.04877	C_{17}(p.u.)	0.04550	0.05000	0.04610
V_{G11}(p.u.)	1.05856	0.97857	1.02193	C_{20}(p.u.)	0.04150	0.04820	0.03720
V_{G13}(p.u.)	1.05555	0.96881	1.01267	C_{21}(p.u.)	0.04930	0.04940	0.04830
$T_{6\text{-}9}$	1.09290	1.00800	1.08050	C_{23}(p.u.)	0.01910	0.04210	0.03070
$T_{6\text{-}10}$	0.90000	0.98800	0.91080	C_{24}(p.u.)	0.04990	0.05000	0.04990
$T_{4\text{-}12}$	1.02610	1.02100	1.01300	C_{29}(p.u.)	0.02270	0.02130	0.02650
$T_{28\text{-}27}$	0.96910	0.97190	0.97690				
				$\boldsymbol{P_{loss}}$ **(p.u.)**	0.051358	0.051348	**0.051337**
				$\boldsymbol{V_d}$ **(p.u.)**	0.301026	0.291872	**0.281155**

TABLE III SIMULATION RESULTS OF BCS OF CASE2

Control Variables	MOICA-I	MOICA-II	MOICA-III	Control Variables	MOICA-I	MOICA-II	MOICA-III
V_{G1}(p.u.)	0.95000	1.05360	0.97261	C_{10}(p.u.)	0.04990	0.04950	0.05000
V_{G2}(p.u.)	0.97196	1.07918	0.97736	C_{12}(p.u.)	0.04820	0.05000	0.04990
V_{G5}(p.u.)	1.00200	0.95877	1.05608	C_{15}(p.u.)	0.04610	0.04800	0.04980
V_{G8}(p.u.)	0.95345	0.95527	1.03700	C_{17}(p.u.)	0.05000	0.04980	0.05000
V_{G11}(p.u.)	0.95862	1.08566	1.03250	C_{20}(p.u.)	0.04960	0.04970	0.04990
V_{G13}(p.u.)	0.95000	1.09856	0.96509	C_{21}(p.u.)	0.04840	0.04980	0.05000
$T_{6\text{-}9}$	0.98820	0.97730	0.98120	C_{23}(p.u.)	0.04210	0.04920	0.04860
$T_{6\text{-}10}$	0.90570	0.90000	0.90000	C_{24}(p.u.)	0.05000	0.04850	0.05000
$T_{4\text{-}12}$	0.95650	0.94850	0.94110	C_{29}(p.u.)	0.04370	0.04180	0.04100
$T_{28\text{-}27}$	0.91920	0.91870	0.91910				
				$\boldsymbol{P_{loss}}$ **(p.u.)**	0.051390	0.051377	**0.051365**
				L index	0.121174	0.120785	**0.120781**

TABLE IV COMPARISONS OF THE OBTAINED MP, ML AND BCS WITH REPORTED MOCIPSO ALGORITHM FOR CASE2

Control Variables	MOICA-III			MOCIPSO [30]		
	MP	ML	BCS	MP	ML	BCS
V_{G1}(p.u.)	0.97664	0.96619	0.97261	1.10000	1.10000	1.10000
V_{G2}(p.u.)	0.99920	1.00737	0.97736	1.10000	1.10000	1.10000
V_{G5}(p.u.)	1.04310	1.04506	1.05608	1.10000	1.10000	1.10000
V_{G8}(p.u.)	0.96361	1.03457	1.03700	1.10000	0.94002	1.10000
V_{G11}(p.u.)	0.98510	1.01989	1.03250	1.10000	1.10000	1.10000
V_{G13}(p.u.)	0.96641	0.95657	0.96509	0.90000	1.10000	1.10000
$T_{6\text{-}9}$	1.01730	0.92640	0.98120	0.94000	0.98000	0.94000
$T_{6\text{-}10}$	0.90000	0.90000	0.90000	1.08000	1.10000	1.10000
$T_{4\text{-}12}$	0.97250	0.91800	0.94110	1.10000	1.10000	1.10000
$T_{28\text{-}27}$	0.95210	0.90000	0.91910	0.97000	0.94000	0.94000
C_{10}(p.u.)	0.05000	0.05000	0.05000	0.06000	0.30000	0.22000
C_{12}(p.u.)	0.04980	0.04980	0.04990	0.30000	0.30000	0.30000
C_{15}(p.u.)	0.05000	0.05000	0.04980	0.07000	0.20000	0.12000
C_{17}(p.u.)	0.05000	0.05000	0.05000	0.06000	0.13000	0.09000
C_{20}(p.u.)	0.05000	0.04990	0.04990	0.00000	0.00000	0.00000
C_{21}(p.u.)	0.05000	0.04960	0.05000	0.12000	0.18000	0.11000
C_{23}(p.u.)	0.03980	0.04960	0.04860	0.03000	0.02000	0.01000
C_{24}(p.u.)	0.05000	0.05000	0.05000	0.07000	0.09000	0.07000
C_{29}(p.u.)	0.02920	0.05000	0.04100	0.03000	0.00000	0.03000
$\boldsymbol{P_{loss}}$ **(p.u.)**	**0.050920**	0.052324	**0.051365**	**0.05174**	0.05419	**0.05232**
L index	0.127554	**0.116792**	**0.120781**	0.12664	**0.11411**	**0.11821**

MP: minimum P_{loss}; ML: minimum *L index*; BCS: best compromise solution.

TABLE V SIMULATION RESULTS OF BCS OF CASE3

Control Variables	MOICA-I	MOICA-II	MOICA-III	Control Variables	MOICA-I	MOICA-II	MOICA-III
V_{G1}(p.u.)	1.08691	1.09235	1.00584	C_{10}(p.u.)	0.01030	0.01150	0.04620
V_{G2}(p.u.)	1.01105	1.05319	0.96243	C_{12}(p.u.)	0.04400	0.02990	0.02920
V_{G5}(p.u.)	1.07198	1.00457	1.07893	C_{15}(p.u.)	0.04330	0.04210	0.00860
V_{G8}(p.u.)	1.01538	1.05829	1.00169	C_{17}(p.u.)	0.03710	0.01880	0.04450
V_{G11}(p.u.)	0.95000	1.10000	1.02883	C_{20}(p.u.)	0.03120	0.04810	0.04160
V_{G13}(p.u.)	1.04979	1.09434	0.99787	C_{21}(p.u.)	0.04970	0.04090	0.04090
$T_{6\text{-}9}$	1.03980	1.10000	1.09230	C_{23}(p.u.)	0.00740	0.02870	0.01930
$T_{6\text{-}10}$	0.97250	0.90000	0.94500	C_{24}(p.u.)	0.03650	0.03930	0.04950
$T_{4\text{-}12}$	1.07470	1.09850	1.07390	C_{29}(p.u.)	0.05000	0.04850	0.04360
$T_{28\text{-}27}$	0.90000	0.90000	0.90000				
				$\boldsymbol{V_d}$ **(p.u.)**	0.445009	0.432550	**0.427348**
				L index	0.123558	0.123424	**0.123288**

C. *Results for system 2*

1) *Case4: Optimizing P_{loss} and V_d*

In Case4, the proposed three improved methods are tested for simultaneous minimization of P_{loss} and V_d. The results of simulation on the system 2 is a series of dominant solutions are presented in Fig. 11-12. TABLE VI shows a comparison of optimal BCSs of those proposed method, it is observed that MOICA-III has the best BCS among these two algorithms. The proposed MOICA-III algorithm finds 0.2709848 p.u. active power losses and 0.8620723 p.u. voltage deviation for MOORPD problem, the MOICA-II method finds 0.2710686 p.u. and 0.8691996 p.u., and the MOICA-I method finds 0.27113235 p.u. and 0.8764507 p.u., respectively. Therefore, the proposed methods are valid on system 2 and the MOICA-III has the best performance in this optimization experiment.

2) Case5: Optimizing P_{loss} and L index

In Case5, the Pareto fronts obtained from 30 simulation runs for proposed methods are shown in the Fig. 13-14. It is clear that the Pareto front obtained using MOICA-III are superior as compared to the same obtained using MOICA-II and MOICA-I from Fig. 13. The BCSs of improved algorithms acquired from the minimization of P_{loss} and *L index* by using MOICA-I, MOICA-II and MOICA-III have been summed up in TABLE VII. The BCSs are selected as (0.2692880 p.u. and 0.2206386), (0.2692067p.u. and 0.2196037) and (0.2691803 p.u. and 0.2192921) for MOICA-I, MOICA-II and MOICA-III methods, respectively. It can be seen from TABLE VIII that the MP, ML and BCS obtained by MOICA-III are better than the reported MOCIPSO algorithm. This proves the superiority of MOICA-III, especially on the large scale system.

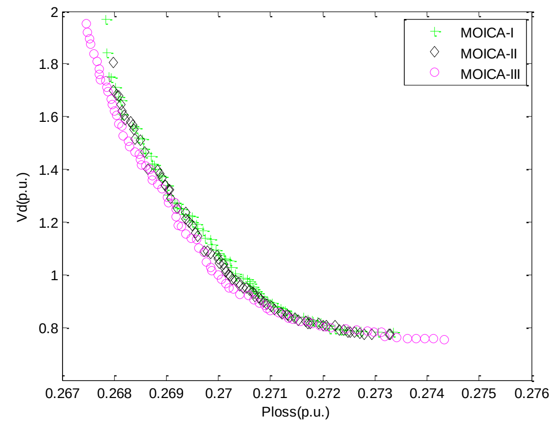

Fig. 11. Simulation results obtained for case4 using of MOICA-I, MOICA-II, MOICA-III

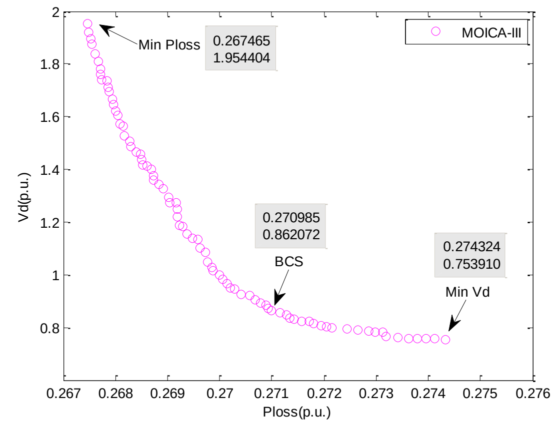

Fig. 12. Pareto optimal fronts of MOICA-III in case4

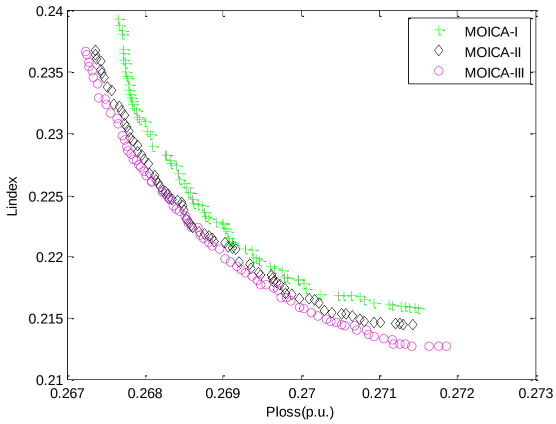

Fig. 13. Simulation results obtained for case5 using of MOICA-I, MOICA-II, MOICA-III

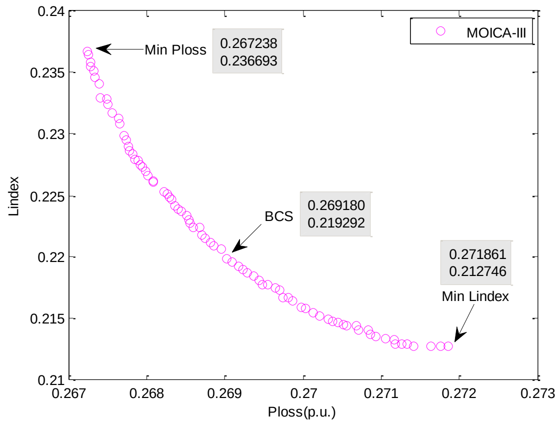

Fig. 14. Pareto optimal fronts of MOICA-III in case5

TABLE VI SIMULATION RESULTS OF BCS OF CASE4

Control Variables	MOICA-I	MOICA-II	MOICA-III	Control Variables	MOICA-I	MOICA-II	MOICA-III
V_{G1}(p.u.)	1.00231	1.07187	1.07829	$T_{34\text{-}32}$	0.93660	0.94000	0.94670
V_{G2}(p.u.)	1.05097	1.02193	1.01753	$T_{11\text{-}41}$	0.90270	0.90040	0.90110
V_{G3}(p.u.)	0.97822	0.95911	1.05428	$T_{15\text{-}45}$	0.93380	0.92600	0.93520
V_{G6}(p.u.)	1.06342	1.08940	1.02174	$T_{14\text{-}46}$	0.93840	0.93540	0.93320
V_{G8}(p.u.)	0.99202	1.02243	1.03569	$T_{10\text{-}51}$	0.95200	0.94960	0.95340
V_{G9}(p.u.)	1.01933	1.05265	1.06556	$T_{13\text{-}49}$	0.91760	0.90680	0.90700
V_{G12}(p.u.)	1.07702	0.96961	1.00955	$T_{11\text{-}43}$	0.90120	0.90690	0.90090
$T_{4\text{-}18}$	1.00540	0.93150	1.03980	$T_{40\text{-}56}$	0.98490	1.01040	1.01820
$T_{4\text{-}18}$	0.93050	0.97630	0.90640	$T_{39\text{-}57}$	0.95640	0.95500	0.95460
$T_{21\text{-}20}$	1.00640	1.00660	0.99940	$T_{9\text{-}55}$	0.93780	0.94760	0.94680
$T_{24\text{-}25}$	0.93820	0.99660	0.97080	C_{18}(p.u.)	0.05450	0.01960	0.03380
$T_{24\text{-}25}$	1.04090	0.95860	1.02320	C_{25}(p.u.)	0.06670	0.05190	0.08480
$T_{24\text{-}26}$	1.00730	1.00930	1.01300	C_{53}(p.u.)	0.04700	0.06210	0.06530
$T_{7\text{-}29}$	0.95190	0.95730	0.95970				
				P_{loss} (p.u.)	0.271132	0.271069	**0.270985**
				V_d (p.u.)	0.876451	0.869200	**0.862072**

TABLE VII SIMULATION RESULTS OF BCS OF CASE5

Control Variables	MOICA-I	MOICA-II	MOICA-III	Control Variables	MOICA-I	MOICA-II	MOICA-III
V_{G1}(p.u.)	1.03077	1.08012	1.06458	$T_{34\text{-}32}$	0.92880	0.94150	0.93560
V_{G2}(p.u.)	1.00935	0.99046	1.09549	$T_{11\text{-}41}$	0.90080	0.90000	0.90520
V_{G3}(p.u.)	0.96182	0.97445	0.98139	$T_{15\text{-}45}$	0.90010	0.90160	0.90130
V_{G6}(p.u.)	0.96459	1.00408	0.95351	$T_{14\text{-}46}$	0.90060	0.90000	0.90040
V_{G8}(p.u.)	0.95030	0.96318	1.02440	$T_{10\text{-}51}$	0.90360	0.90680	0.90440
V_{G9}(p.u.)	1.04953	0.99530	0.96339	$T_{13\text{-}49}$	0.90000	0.90000	0.90000
V_{G12}(p.u.)	1.08134	0.99629	1.04777	$T_{11\text{-}43}$	0.90130	0.90010	0.90850
$T_{4\text{-}18}$	0.90010	0.99020	0.92600	$T_{40\text{-}56}$	1.03700	1.05370	1.09020
$T_{4\text{-}18}$	1.02330	0.90460	0.90090	$T_{39\text{-}57}$	1.00030	1.02850	1.02750
$T_{21\text{-}20}$	1.06550	1.01820	1.00630	$T_{9\text{-}55}$	0.90160	0.90170	0.90000
$T_{24\text{-}25}$	1.10000	1.08600	1.06370	C_{18}(p.u.)	0.05180	0.07120	0.00000
$T_{24\text{-}25}$	1.05760	1.07660	1.08540	C_{25}(p.u.)	0.20840	0.21650	0.21100
$T_{24\text{-}26}$	1.01850	1.01390	0.99060	C_{53}(p.u.)	0.03520	0.03580	0.01380
$T_{7\text{-}29}$	0.93200	0.92750	0.91310				
				P_{loss} (p.u.)	0.269288	0.269207	**0.269180**
				L index	0.220639	0.219604	**0.219292**

TABLE VIII COMPARISONS OF THE OBTAINED MP, ML AND BCS WITH REPORTED MOCIPSO ALGORITHM FOR CASE5

Control Variables	MOICA-III			MOCIPSO [30]		
	MP	ML	BCS	MP	ML	BCS
V_{G1}(p.u.)	0.98007	1.02788	1.06458	0.90000	0.90000	1.10000
V_{G2}(p.u.)	1.03577	1.01564	1.09549	1.04996	0.90000	0.93520
V_{G3}(p.u.)	0.96458	0.95000	0.98139	1.10000	0.93820	0.90000
V_{G6}(p.u.)	1.00469	0.95002	0.95351	0.99769	0.90831	0.90000
V_{G8}(p.u.)	0.96811	0.96966	1.02440	0.90000	1.10000	1.07345
V_{G9}(p.u.)	0.95340	0.99874	0.96339	0.90000	1.10000	0.90000
V_{G12}(p.u.)	0.95098	0.95173	1.04777	1.01203	1.08472	0.96240
$T_{4\text{-}18}$	0.90000	0.90320	0.92600	0.96000	0.96000	0.96000
$T_{4\text{-}18}$	0.90130	0.90060	0.90090	0.90000	0.90000	0.90000
$T_{21\text{-}20}$	1.00210	1.00450	1.00630	1.00000	1.00000	1.01000
$T_{24\text{-}25}$	1.09880	1.09970	1.06370	1.10000	1.10000	1.10000
$T_{24\text{-}25}$	0.91610	1.10000	1.08540	1.10000	1.10000	1.10000
$T_{24\text{-}26}$	0.99940	0.96460	0.99060	1.00000	1.02000	1.01000
$T_{7\text{-}29}$	0.91050	0.91200	0.91310	0.93000	0.93000	0.93000
$T_{34\text{-}32}$	0.93620	0.90000	0.93560	0.98000	0.90000	0.93000
$T_{11\text{-}41}$	0.90080	0.90000	0.90520	0.97000	0.94000	0.96000
$T_{15\text{-}45}$	0.90000	0.90060	0.90130	0.94000	0.94000	0.94000
$T_{14\text{-}46}$	0.90020	0.90010	0.90040	0.92000	0.92000	0.92000
$T_{10\text{-}51}$	0.90830	0.90000	0.90440	0.93000	0.93000	0.93000
$T_{13\text{-}49}$	0.90000	0.90000	0.90000	0.90000	0.90000	0.90000
$T_{11\text{-}43}$	0.90040	0.90000	0.90850	0.90000	0.90000	0.90000
$T_{40\text{-}56}$	1.05030	1.08280	1.09020	1.08000	1.10000	1.08000
$T_{39\text{-}57}$	1.00600	1.06950	1.02750	1.00000	1.05000	1.02000
$T_{9\text{-}55}$	0.90000	0.90000	0.90000	0.92000	0.92000	0.92000
C_{18}(p.u.)	0.00070	0.05290	0.00000	0.00000	0.00000	0.00000
C_{25}(p.u.)	0.11090	0.24150	0.21100	0.18000	0.18000	0.18000
C_{53}(p.u.)	0.02300	0.01980	0.01380	0.04200	0.05400	0.04800
P_{loss} (p.u.)	**0.267238**	0.271861	**0.269180**	**0.27075**	0.27254	**0.27122**
L index	0.236693	**0.212746**	**0.219292**	0.24274	**0.23291**	**0.23695**

MP: minimum P_{loss}; ML: minimum *L index*; BCS: best compromise solution.

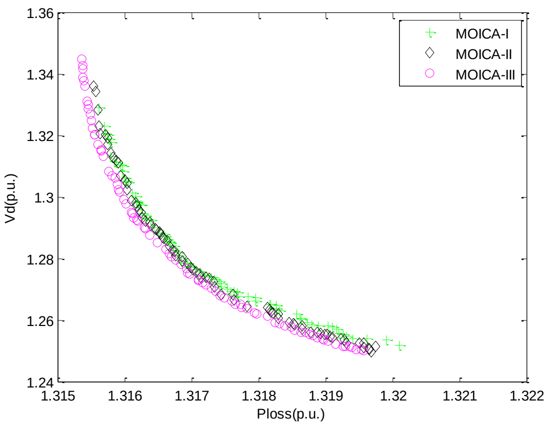

Fig. 15. Simulation results obtained for case6 using of MOICA-I, MOICA-II, MOICA-III

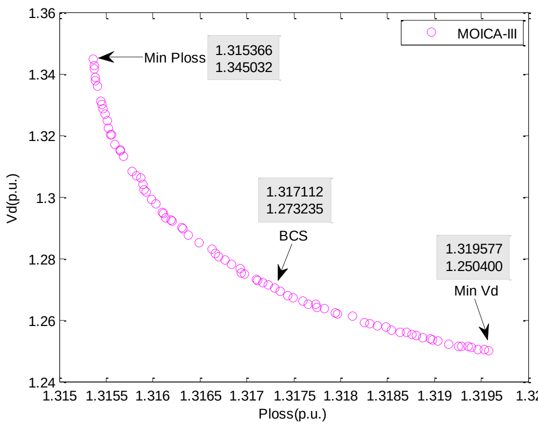

Fig. 16. Pareto optimal fronts of MOICA-III in case6

D. Results for system 3

1) Case6: Optimizing P_{loss} and V_d

In order to find the Pareto front in the larger IEEE118 bus test system, we apply the proposed method to simultaneous minimization of IEEE118 bus test system with active power losses and voltage deviation. It is inferred from this Fig. 15 that the results obtained by the MOICA-I, MOICA-II and MOICA-III are very close, which means the fact that those proposed methods are effective on large bus system. Fig. 16 shows the minimum P_{loss}, minimum V_d and BCS of MOICA-III in the system 3. It can be seen that the minimum P_{loss} is 1.315366 p.u. and the minimum V_d is 1.250400 p.u.. A more detailed comparison of the results of the BCS of the MOICA-I, MOICA-II and MOICA-III is shown in TABLE IX. It is notable that the MOICA-III find the lower active power losses and less voltage deviation than MOICA-I and MOICA-II.

TABLE IX SIMULATION RESULTS OF BCS OF CASE6

Control Variables	MOICA-I	MOICA-II	MOICA-III	Control Variables	MOICA-I	MOICA-II	MOICA-III
V_{G1}(p.u.)	1.09948	0.90000	0.92634	V_{G87}(p.u.)	1.10000	1.10000	0.91168
V_{G4}(p.u.)	1.09939	1.03550	1.07995	V_{G89}(p.u.)	1.09387	0.91014	0.98920
V_{G6}(p.u.)	1.10000	1.09559	1.06341	V_{G90}(p.u.)	1.10000	1.10000	0.95425
V_{G8}(p.u.)	1.09270	1.10000	0.95486	V_{G91}(p.u.)	1.09291	1.10000	1.00979
V_{G10}(p.u.)	0.93466	1.10000	0.92722	V_{G92}(p.u.)	1.09621	1.10000	0.92335
V_{G12}(p.u.)	0.90000	0.90000	1.03155	V_{G99}(p.u.)	1.10000	0.90037	1.08149
V_{G15}(p.u.)	0.90000	0.91706	0.98782	V_{G100}(p.u.)	1.08972	0.90000	0.99429
V_{G18}(p.u.)	1.10000	1.10000	1.03561	V_{G103}(p.u.)	0.90000	1.10000	1.01720
V_{G19} (p.u.)	0.92788	1.10000	1.01682	V_{G104}(p.u.)	1.09874	1.10000	1.07246
V_{G24}(p.u.)	1.03514	1.10000	0.96372	V_{G105}(p.u.)	1.09993	0.95894	0.93417
V_{G25}(p.u.)	0.95700	1.08538	0.91777	V_{G107}(p.u.)	1.04879	0.90318	0.99250
V_{G26}(p.u.)	0.90000	1.08215	0.95305	V_{G110}(p.u.)	0.90000	1.10000	1.01990
V_{G27}(p.u.)	0.90000	1.10000	0.95578	V_{G111}(p.u.)	0.90563	1.09998	1.03521
V_{G31}(p.u.)	1.09633	0.93390	0.96054	V_{G112}(p.u.)	1.10000	0.90000	1.06835
V_{G32}(p.u.)	0.96673	0.90000	0.94240	V_{G113}(p.u.)	0.94220	0.90000	1.07848
V_{G34}(p.u.)	1.06267	0.90000	0.97807	V_{G116}(p.u.)	1.10000	1.09922	1.07102
V_{G36}(p.u.)	1.05093	0.92974	1.09279	T_8	0.99560	0.99080	0.99400
V_{G40}(p.u.)	1.09213	0.91248	1.07222	T_{32}	0.97820	0.99050	0.99030
V_{G42}(p.u.)	0.90000	1.10000	1.06275	T_{36}	0.99980	0.99390	0.99720
V_{G46}(p.u.)	0.90000	1.10000	1.04710	T_{51}	0.99490	0.99560	0.99790
V_{G49}(p.u.)	0.90000	0.90000	1.00582	T_{93}	1.01240	1.01490	1.01510
V_{G54}(p.u.)	0.90008	0.90000	0.98921	T_{95}	1.00390	1.00180	0.99730
V_{G55}(p.u.)	1.05198	0.90460	0.92659	T_{102}	0.96270	0.96690	0.92640
V_{G56}(p.u.)	1.09322	0.90000	1.01045	T_{107}	0.90880	0.90420	0.91200
V_{G59}(p.u.)	1.09833	0.90616	1.02265	T_{127}	0.94570	0.94650	0.94490
V_{G61}(p.u.)	1.07236	1.09999	1.00135	C_{34}(p.u.)	0.11170	0.22190	0.29560
V_{G62}(p.u.)	1.04545	0.90000	1.00131	C_{44}(p.u.)	0.11340	0.10590	0.14790
V_{G65}(p.u.)	0.90219	0.90000	0.90500	C_{45}(p.u.)	0.30000	0.30000	0.24840
V_{G66}(p.u.)	1.02185	0.91474	1.07770	C_{46}(p.u.)	0.29990	0.00000	0.06980
V_{G69}(p.u.)	0.99293	1.10000	0.90107	C_{48}(p.u.)	0.01320	0.02020	0.00980
V_{G70}(p.u.)	1.08738	0.94539	0.91042	C_{74}(p.u.)	0.28770	0.29460	0.00290
V_{G72}(p.u.)	1.08260	0.91005	0.98407	C_{79}(p.u.)	0.18710	0.24970	0.22320
V_{G73}(p.u.)	1.10000	0.90000	0.94113	C_{82}(p.u.)	0.30000	0.29920	0.29730
V_{G74}(p.u.)	1.02150	1.10000	1.02230	C_{83}(p.u.)	0.29640	0.30000	0.27450
V_{G76}(p.u.)	1.10000	0.90389	1.02562	C_{105}(p.u.)	0.00000	0.00000	0.21610
V_{G77}(p.u.)	1.09112	0.90036	0.99291	C_{107}(p.u.)	0.00000	0.10020	0.16130
V_{G80}(p.u.)	0.90000	0.91116	0.99592	C_{110}(p.u.)	0.13400	0.00010	0.15320
V_{G85}(p.u.)	0.91601	0.90000	0.94579				
			P_{loss} (p.u.)		1.317178	1.317221	**1.317112**
			V_d (p.u.)		1.274844	1.274244	**1.273235**

E. Performance evaluation

Performance indicators are used to evaluate whether the algorithm achieves the desired goals. Hence, in order to further evaluate the performance of the MOICA-I, MOICA-II and MOICA-III algorithms, two indicators were selected: Generational Distance (*GD*) indicator and Hyper-volume (*HV*) indicator.

1) GD

The *GD* indicator is used to describe the distance between the dominant solution obtained by the algorithm and the true Pareto front of the problem. In different cases of this test experiment, the best one Pareto front obtained by using above proposed methods, and this best one Pareto front is considered the true Pareto front. For the true Pareto front, its *GD* is equal to 0. This means that the smaller the *GD* is, the closer all the generated countries are to the true Pareto front. *GD* can be expressed by (31).

$$GD = \frac{\sqrt{\sum_{i=1}^{n} d_i^2}}{n} \tag{31}$$

where n represents the total amount of the solutions, d_i represents the shortest distance between the ith solution and the true Pareto front.

2) HV

The *HV* indicator is used to calculate the volume of non-dominated solution set obtained by the optimization algorithm. *HV* is an effective one-dimensional quality metric. It is strictly monotonous in terms of Pareto dominance. The larger the value of *HV* is, the better performance of the corresponding algorithm. The mathematical formula for *HV* is shown as follows:

$$HV = \delta(\bigcup_{i=1}^{|S|} v_i) \tag{32}$$

where δ represents the Lebesgue measure which is used to measure volume [35], $|S|$ indicates the number of non-dominated solution sets and v_i denotes the volume formed by reference point and the ith solution.

3) Statistical analysis

In this section, we will use the boxplot to analyze the *GD* and *HV* indicators. This method is a statistical graph used to display the dispersion of a set of data. The detail data includes: maximum, minimum, median, outlier, upper quartile and lower quartile. For the *GD* indicator, the best one optimal Pareto front is chosen as the true Pareto front in different cases. The box plots of *GD* and *HV* for MOICA-I, MOICA-II and MOICA-III among Cases 1-6 are shown as Fig. 17. The results of the *GD* indicator shows that the MOICA-III algorithm has a lower value than the results of the other two algorithms, which indicates that the result of each iteration of the algorithm is closer to the true Pareto front. It can be seen from Fig. 18 that the *HV* indicator of MOICA-III is higher than that of the other two algorithms, which also shows the superiority of MOICA-III.

In order to further observe the performance of the above indicators, TABLE X lists the mean and standard deviation values of the *GD* and *HV* indicators in Cases 1-6. As seen in the TABLE X, in both *GD* and *HV* indicators, the mean value and standard deviation values of the MOICA-III are better than those of the other two methods. It is also indicates that MOICA-III has certain competitive advantages in those cases and can obtain solutions with better diversity.

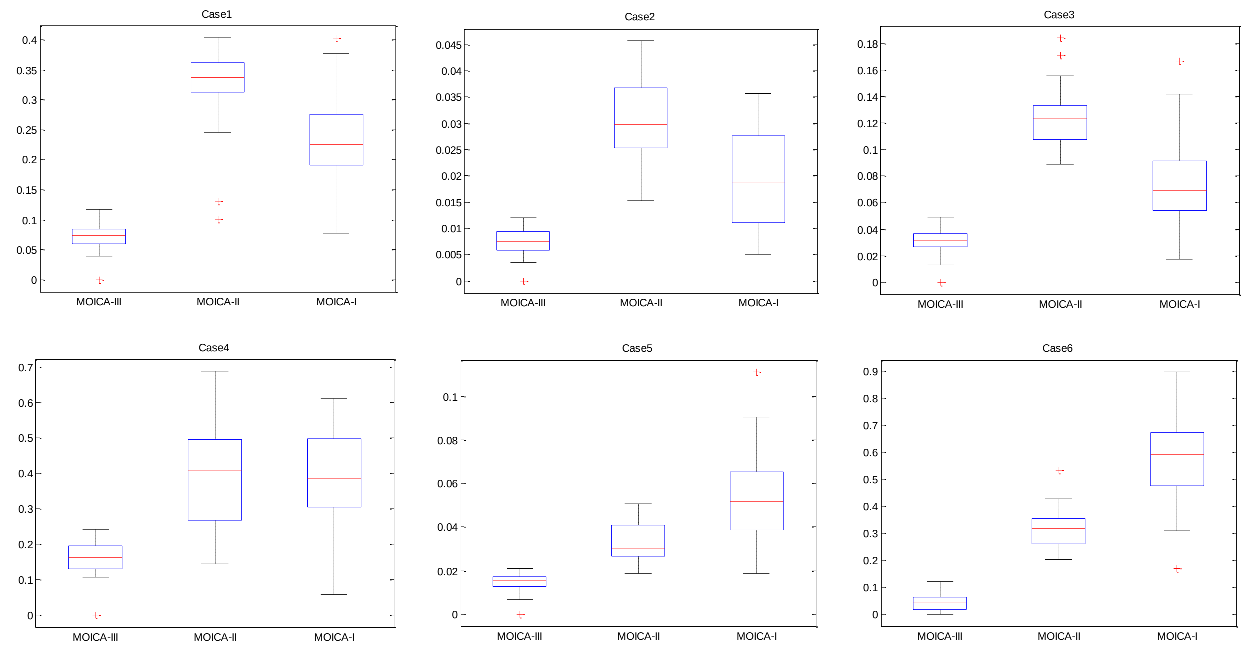

Fig. 17. Box plots of *GD* for the MOICA-I, MOICA-II and MOICA-III

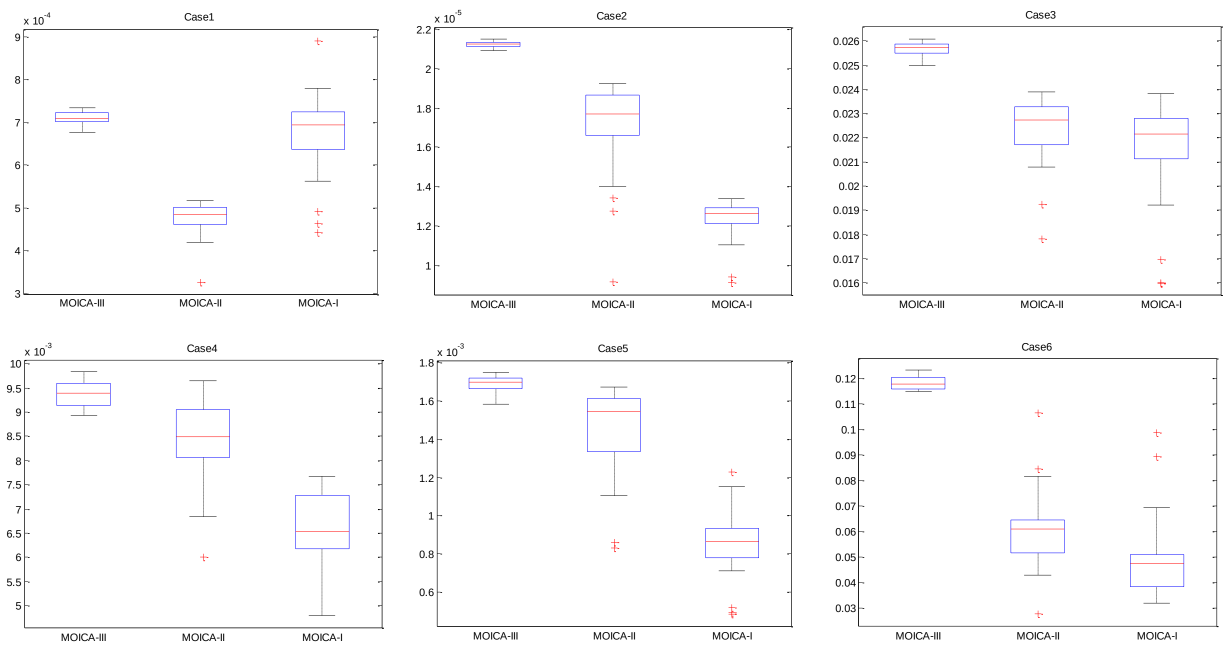

Fig. 18. Box plots of *HV* for the MOICA-I, MOICA-II and MOICA-III

TABLE X The mean and standard deviation of *GD* and *HV* for the MOICA-I, MOICA-II and MOICA-III

Indicator	Test Case	MOICA-III		MOICA-II		MOICA-I	
		Mean	Std	Mean	Std	Mean	Std
GD	Case1	0.07258	0.02291	0.33045	0.05631	0.23099	0.08062
	Case2	0.00759	0.00277	0.03050	0.00738	0.01927	0.00890
	Case3	0.03062	0.01043	0.12404	0.02268	0.07410	0.03690
	Case4	0.15963	0.04843	0.39934	0.14826	0.38819	0.14149
	Case5	0.01439	0.00432	0.03276	0.00912	0.05323	0.02036
	Case6	0.04362	0.02828	0.31062	0.07342	0.56900	0.17790
HV	Case1	0.00071	1.45E-05	0.00048	3.75E-05	0.00067	9.53E-05
	Case2	2.12E-05	1.54E-07	1.72E-05	2.28E-06	1.24E-05	1.01E-06
	Case3	0.02568	0.00027	0.02231	0.00133	0.02155	0.00204
	Case4	0.00937	0.00025	0.00842	0.00081	0.00656	0.00078
	Case5	0.00169	4.23E-05	0.00145	0.00023	0.00086	0.00017
	Case6	0.11814	0.00244	0.06045	0.01542	0.04989	0.01620

Mean: mean value; Std: standard deviation value.

V. CONCLUSION

There are three main problems in solving the MOORPD problem by using the ICA method: the application of ICA in the MOPs, the processing method of constraints, and the measurement method of the quality of the solution. In view of the above-mentioned problems, this paper proposes three enhanced MOICAs, namely MOICA-I, MOICA-II and MOICA-III. The simulation experiments of enhanced approaches in three test systems (the IEEE 30, 57 and 118 bus systems) verify their effectiveness in dealing with MOORPD problem. Compared with MOICA-I and MOICA-II, the Pareto plots and the results of BCS show that the MOICA-III method is much more effective and can obtain the better Pareto solutions. In addition, from the *GD* and *HV* indicators of the three approaches, it is clear that the stability, diversity and optimization results of MOICA-III were superior to the other two approaches.

ACKNOWLEDGEMENTS

The authors would like to thank the editors and the reviewers for their constructive comments and suggestions.

REFERENCES

[1] G. Chen, Z. Lu, Z. Zhang, and Z. Sun, "Research on hybrid modified cuckoo search algorithm for optimal reactive power dispatch problem," *IAENG International Journal of Computer Science,* vol. 45, no. 2, pp. 328-339, 2018.

[2] S. Dutta, S. Paul and P. K. Roy, "Optimal allocation of SVC and TCSC using quasi-oppositional chemical reaction optimization for solving multi-objective ORPD problem," *Journal of Electrical Systems and Information Technology,* vol. 5, no. 1, pp. 83-98, 2018.

[3] G. Chen, J. Qian, Z. Zhang, and Z. Sun, "Multi-objective improved bat algorithm for optimizing fuel cost, emission and active power loss in power system," *IAENG International Journal of Computer Science*, vol. 46, no. 1, pp. 118-133, 2019.

[4] R. Ng Shin Mei, M. H. Sulaiman, Z. Mustaffa, and et al, "Optimal reactive power dispatch solution by loss minimization using moth-flame optimization technique," *Applied Soft Computing,* vol. 59, pp. 210-222, 2017.

[5] S. Mouassa, T. Bouktir and A. Salhi, "Ant lion optimizer for solving optimal reactive power dispatch problem in power systems," *Engineering Science and Technology, an International Journal,* vol. 20, no. 3, pp. 885-895, 2017.

[6] A. Saraswat and A. Saini, "Multi-objective optimal reactive power dispatch considering voltage stability in power systems using HFMOEA," *Engineering Applications of Artificial Intelligence,* vol. 26, no. 1, pp. 390-404, 2013.

[7] A. Ghasemi, K. Valipour and A. Tohidi, "Multi objective optimal reactive power dispatch using a new multi objective strategy," *International Journal of Electrical Power & Energy Systems,* vol. 57, pp. 318-334, 2014.

[8] K. Nuaekaew, P. Artrit, N. Pholdee, and et al, "Optimal reactive power dispatch problem using a two-archive multi-objective grey wolf optimizer," *Expert Systems with Applications,* vol. 87, pp. 79-89, 2017.

[9] G. Sauvanet and E. Néron, "Search for the best compromise solution on Multiobjective shortest path problem," *Electronic Notes in Discrete Mathematics,* vol. 36, pp. 615-622, 2010.

[10] J. L. Cohon, Multiobjective Programming and Planning, Academic Press, 1978.

[11] J. Xiong, C. Liu, Y. Chen, and S. Zhang, "A non-linear geophysical inversion algorithm for the mt data based on improved differential evolution", *Engineering Letters*, vol. 26, no. 1, pp. 161-170, 2018.

[12] M. George, "Effective implementation of the ε-constraint method in Multi-Objective Mathematical Programming problems," *Applied Mathematics & Computation,* vol. 213, no. 2, pp. 455-465, 2009.

[13] Y. L. Chen and C. C. Liu, "Multiobjective VAr planning using the goal-attainment method," *IET Proceedings - Generation Transmission and Distribution,* vol. 141, pp. 227-232, 1994.

[14] K. Deb, A. Pratap, S. Agarwal, and et al, "A fast and elitist multiobjective genetic algorithm: NSGA-II," *IEEE Transactions on Evolutionary Computation,* vol. 6, pp. 182-197, 2002.

[15] Li S, Jiao L, Zhang Y, et al. "A scheme of resource allocation for heterogeneous services in peer-to-peer networks using particle swarm optimization," *IAENG International Journal of Computer Science*, vol.44, no.4, pp.482-488, 2017.

[16] B. Gadhvi, V. Savsani and V. Patel, "Multi-objective optimization of vehicle passive suspension system using NSGA-II, SPEA2 and PESA-II," *Procedia Technology,* vol. 23, pp. 361-368, 2016.

[17] E. Atashpaz-Gargari and C. Lucas, "Imperialist competitive algorithm: An algorithm for optimization inspired by imperialistic competition," in *IEEE Congress on Evolutionary Computation*, 2008.

[18] M. R. Maheri and M. Talezadeh, "An Enhanced Imperialist Competitive Algorithm for optimum design of skeletal structures," *Swarm and Evolutionary Computation,* vol. 40, pp. 24-36, 2018.

[19] R. Enayatifar, M. Yousefi, A. H. Abdullah, and et al, "MOICA: A novel multi-objective approach based on imperialist competitive algorithm," *Applied Mathematics and Computation,* vol. 219, no.17, pp. 8829-8841, 2013.

[20] M. Ghasemi, S. Ghavidel, M. M. Ghanbarian, et al. "Multi-objective optimal power flow considering the cost, emission, voltage deviation and power losses using multi-objective modified imperialist competitive algorithm," *Energy,* vol. 78, pp. 276-289, 2014.

[21] M. Ghasemi, S. Ghavidel, M. M. Ghanbarian, and et al, "Multi-objective optimal electric power planning in the power system using

Gaussian bare-bones imperialist competitive algorithm," *Information Sciences,* vol. 294, pp. 286-304, 2015.

[22] S. Hosseini and A. Al Khaled, "A survey on the Imperialist Competitive Algorithm metaheuristic: Implementation in engineering domain and directions for future research," *Applied Soft Computing,* vol. 24, pp. 1078-1094, 2014.

[23] M. Ali Ahmad, M. Ebadi, A. Shokrollahi and et al, "Evolving artificial neural network and imperialist competitive algorithm for prediction oil flow rate of the reservoir," *Applied Soft Computing,* vol. 13, pp. 1085-1098, 2013.

[24] A. K. Sadhu, P. Rakshit and A. Konar, "A modified Imperialist Competitive Algorithm for multi-robot stick-carrying application," *Robotics and Autonomous Systems,* vol. 76, pp. 15-35, 2016.

[25] X. Li, "A Non-dominated Sorting Particle Swarm Optimizer for Multiobjective Optimization," in *Genetic & Evolutionary Computation Conference,* GECCO, 2003.

[26] C. A. C. Coello, G. T. Pulido and M. S. Lechuga, "Handling multiple objectives with particle swarm optimization," *IEEE Transactions on Evolutionary Computation,* vol. 8, pp. 256-279, 2004.

[27] R. L. While, L. Bradstreet and L. Barone, "A fast way of calculating exact hypervolumes," *IEEE Transactions on Evolutionary Computation,* vol. 16, pp. 86-95, 2012.

[28] E. Atashpaz-Gargari and C. Lucas, "Imperialist competitive algorithm: an algorithm for optimization inspired by imperialistic competition," in *IEEE Congress on Evolutionary Computation*, 2008.

[29] K. Y. Lee and Y. M. Park, "A united approach to optimal real and reactive power dispatch," *IEEE Power Engineering Review,* vol. PER-5, pp. 42-43, 2010.

[30] G. Chen, L. Liu, P. Song, and Y. Du, "Chaotic improved PSO-based multi-objective optimization for minimization of power losses and L index in power systems," *Energy Conversion & Management,* vol. 86, pp. 548-560, 2014.

[31] R. D. Zimmerman, C. E. M. Sanchez and D. Gan" MATPOWER: A Matlab Power System Simulation Package," 2007 (accessed 17.02.23) http://www.pserc.cornell.edu/matpower/.

[32] G. Chen, L. Liu, Z. Zhang, and et al, "Optimal reactive power dispatch by improved GSA-based algorithm with the novel strategies to handle constraints," *Applied Soft Computing,* vol. 50, pp. 58-70, 2017.

[33] G. Chen, X. Yi, Z. Zhang, and et al, "Applications of multi-objective dimension-based firefly algorithm to optimize the power losses, emission, and cost in power systems," *Applied Soft Computing,* vol.68, pp.322-342, 2018.

[34] L.F. Zhu, J. S. Wang, "Data clustering method based on bat algorithm and parameters optimization," *Engineering Letters*, vol. 27, no. 1, pp 241-250, 2019.

[35] J. Bader and E. Zitzler, "HypE: an algorithm for fast hypervolume-based many-objective optimization," *Evolutionary Computation,* vol. 19, pp. 45-76, 2011.